Journal of Trace Elements in Medicine and Biology 89 (2025) 127668

Contents lists available at ScienceDirect

Journal of Trace Elements in Medicine and Biology

journal homepage: www.elsevier.com/locate/jtemb

Insights into ionic medicine: Cerium reduces the presence of reactive oxygen species and favors osteogenic over adipogenic differentiation in human mesenchymal stromal cells

F. Westhauser [a,b,*], V. Jacobsen [b], K. Zheng [c], C. Merle [d], A.R. Boccaccini [e], T. Renkawitz [a,b], E. Kunisch [b]

[a] Department of Orthopaedics, Regensburg University Medical Center, Asklepios Klinikum Bad Abbach, Kaiser-Karl V.-Allee 3, Bad Abbach 93077, Germany
[b] Department of Orthopedics, Heidelberg University Hospital, Schlierbacher Landstraße 200a, Heidelberg 69118, Germany
[c] Engineering Research Center of Stomatological Translational Medicine, Nanjing Medical University, 136 Hanzhong Rd., Nanjing 210029, China
[d] Joint Replacement Centre, Orthopedic Surgery Paulinenhilfe, Diakonie-Klinikum Stuttgart, Rosenbergstraße 38, Stuttgart 70176, Germany
[e] Institute of Biomaterials, University of Erlangen-Nuremberg, Cauerstraße 6, Erlangen 91058, Germany

ARTICLE INFO

Keywords:
Cerium
Human bone marrow derived mesenchymal stromal cells
Adipogenesis
Osteogenesis
Viability
Proliferation
Reactive oxygen species

ABSTRACT

The guided application of metallic ions in bone tissue engineering (BTE) has recently gained popularity being described as one important example of ionic medicine (IM). BTE aims to enhance osteogenic differentiation of precursor cells like bone-marrow-derived mesenchymal stromal cells (BMSCs) and, by that, regenerate bone tissue. BMSCs however can also differentiate into adipogenic lineage. It is known that elevated levels of reactive oxygen species (ROS) stimulate BMSC towards (undesired) adipogenic differentiation. One ion, that is particularly interesting for application in IM-guided BTE is cerium (Ce) since it acts as a self-regenerating ROS-scavenger and has already been successfully incorporated in biomaterials. Ce has demonstrated pro-osteogenic, anti-adipogenic and anti-oxidative effects before, however, so far, there is no direct comparative study available that analyzes these effects on human BMSCs in one and the same setting. Therefore, in this study, the influence of Ce nitrate (CeN) on the expression of osteogenic, adipogenic and ROS-scavenging genes in BMSCs was evaluated as well as its impact on formation of an osseous extracellular matrix (ECM), lipid formation and physical ROS presence. The presence of CeN improved BMSCs viability, enhanced proliferation, and reduced ROS-levels. Furthermore, CeN suppressed adipogenesis while osteogenic differentiation and the formation and maturation of the ECM were enhanced. The presence of CeN reduced the physical presence of ROS and the gene expression patterns shifted towards an anti-oxidant profile. Ce therefore constitutes an attractive ion for application in IM-guided BTE. Further research is necessary to clarify the biological mechanisms and pathways that are involved in the Ce-mediated modulation of BMSC differentiation.

1. Introduction

Musculoskeletal hard and soft tissue regeneration processes can be supported by various approaches, including (but not limited to) the application of biomaterials, stem cells or growth and differentiation factors [1,2]. The concept of "ionic medicine" (IM) has been introduced recently and is gaining increasing attention for tissue engineering applications [1]. IM captures the idea of exploiting the therapeutic potential of metallic and non-metallic biologically active ions that are delivered locally to their anticipated site of action [1]. One variant of IM comprises the targeted application of biologically active ions to regenerate tissue. Especially as a part of biomaterials, such as bioactive glasses (BGs), the addition and local release of metallic ions has become a popular field within both, biomaterials science and (mainly) bone tissue engineering (BTE) [3–5].

A great number of ions have shown biological properties that make them attractive candidates for application in BTE approaches. For example, boron ions as part of BGs have been shown to enhance angiogenesis leading to improved bone tissue formation mediated by an increased availability of nutrients [6]. One ion that recently gained

* Corresponding author at: Department of Orthopaedics, Regensburg University Medical Center, Asklepios Klinikum Bad Abbach, Kaiser-Karl V.-Allee 3, Bad Abbach 93077, Germany.
E-mail address: Fabian.Westhauser@klinik.uni-regensburg.de (F. Westhauser).

https://doi.org/10.1016/j.jtemb.2025.127668
Received 18 February 2025; Received in revised form 21 April 2025; Accepted 30 April 2025
Available online 1 May 2025

particular interest for BTE applications is cerium (Ce). Ce, an element from the lanthanoid group, has been shown to enhance osteogenic differentiation of bone precursor cells such as bone-marrow derived mesenchymal stromal cells (BMSCs) and to act anti-oxidative by modulating reactive oxygen species (ROS) as a part of BGs or nanoparticles [7–11]. The anti-oxidative effects of Ce are linked to its ability to act as a self-regenerating ROS-scavenger [12]. The ROS-modulating properties of Ce are certainly remarkable: since it is known that elevated ROS levels favor adipogenic over osteogenic differentiation of BMSCs, the presence of a ROS-reducing compound might therefore suppress adipogenic and support osteogenic differentiation of BMSCs [13,14]. This makes Ce-containing biomaterials attractive vehicles for IM-approaches in BTE.

While the effects of Ce on adipogenic and osteogenic differentiation as well as the impact on the genetic activity of genes encoding for ROS-scavenging enzymes have already been described [7–12, 15–18], there is, to the authors' best knowledge, no directly comparative study available that analyzes the effects on ROS production, adipogenic and osteogenic differentiation of human BMSCs in one and the same setting. Furthermore, a direct analysis regarding the actual physical presence of ROS in a cultivation setting that involves Ce is not yet available. The available studies mainly use non-human cells to assess the biological actions of Ce [15]. Furthermore, changes that involve the modualation of ROS are solely available on a genetic level while the actual physical presence of ROS has not yet been evaluated [9].

While Ce is available in different biological active molecules such as cerium chloride ($CeCl_2$) [15,16] or cerium oxide [12,19,20], this study evaluated the impact of cerium nitrate ($Ce(NO_3)_3$; CeN) on BMSCs since CeN is a compound commonly used for the synthesis of Ce-doped biomaterials, mainly Ce-doped BGs [7,9,21]. The cytocompatibility of CeN on BMSCs was assessed by monitoring its influence on cell viability and growth. The effects of CeN on BMSCs' osteogenic differentiation were assessed by gene expression analysis, cellular differentiation evaluation and by quantifying the impact on formation and maturation of a primitive, osteogenic extracellular matrix (ECM). Adipogenic differentiation of BMSCs in the presence of CeN was evaluated by quantification of lipid vacuoles and on gene expression level. The evaluation of the impact of CeN on ROS-scavenging enzymes was also analyzed. Furthermore, the physical presence and activity of ROS were assessed.

2. Materials and methods

2.1. Study ethics

The responsible ethics committee of the Medical Faculty of Heidelberg University approved the harvesting of patient tissue samples, isolation and cultivation of cells used for this study (S-340/2018).

2.2. BMSC origin, isolation and cultivation

Tissue samples were obtained from 10 different patients undergoing hip arthroplasty. Five male and five female patients were included with an average age of 63 years (Range: 45–85 years) for the male donors and 65.2 years (Range: 47–78 years) for the female donors. The patients were selected in order to provide a representative basis for the analysis of the biological effects of CeN. It has been shown that pooling of BMSCs reduces the vast inter-individual differences in cellular behavior that is highly dependent on the individual donors [22]. Cells were isolated from the tissue samples following a previously published protocol [23, 24]. Differences between individual variations in cellular behavior were adjusted by pooling the isolated BMSCs in equal parts as previously described [22]. BMSCs were expanded in expansion medium (EM; composition: Dulbecco's modified Eagle's medium (DMEM) high glucose, 12.5 % fetal calf serum (FCS), 2 mM L-glutamine, 1 % non-essential amino acids (NEAA), 50 μM β-mercaptoethanol (all Life Technologies, Darmstadt, Germany), 100 μg/ml penicillin/streptomycin (Sigma Aldrich, Steinheim, Germany) and 4 ng/ml fibroblast growth factor 2 (Active Bioscience, Hamburg, Germany) in 0.1 % gelatin (Sigma Aldrich) coated T175 cell culture flasks (Sarstedt, Nümbrecht, Germany) under standard cell culture conditions (37°C, 5 % CO_2, humified atmosphere). To discard non-adherent cells, EM was changed twice weekly. For experiments, BMSCs in passage 4 were used. It is known for BMSCs that with increasing passage, their differentiation and growth performance decreases [25]. Passage 4 BMSCs were chosen based on our previous experience and data from the literature, since it allows enough time to expand the cells and retains proper osteogenic differentiation potential [22, 25–27].

2.3. Cell culture setting

BMSCs were seeded out in either 12-, 24- or 96 well plates (Sarstedt, Nümbrecht, Germany) in a density of 18.75×10^3 cells/cm^2 in cell culture medium (CCM; composition: DMEM, 10 % fetal calf serum (FCS) and 100 μg/ml penicillin/streptomycin (Sigma Aldrich). Medium was changed two times per week until evaluations were carried out on day 7 (D7) and 14 (D14) for all assays except for ECM analysis – these experiments were carried out on D14 and day 21 (D21) in order to provide the ECM the necessary time to form.

For the analysis on the modulation of adipogenic differentiation, adipogenesis stimulating supplements (0.01 mg/ml insulin glargin (Sanofi, Frankfurt am Main, Germany), 1 μM dexamethasone, 0.2 mM indomethacin and 0.5 mM 3-isobutyl-1-methylxanthine (all Sigma Aldrich)) were added on D1 to the CCM, creating adipogenesis inducing medium (AIM). Subsequent medium changes were performed without adding dexamethasone and 3-isobutyl-1-methylxanthine.

2.4. Addition of CeN to the cell culture media

Cerium nitrate ionic solution was prepared by dissolving $Ce(NO_3)_3$ 6 H_2O (CeN, 99.99 % trace metals basis, Sigma-Aldrich) in distilled water (Life Technologies) and subsequent sterile filtration using Whatman Puradisc 30 mm syringe filters with 0.2 μm pore size (Merck, Darmstadt, Germany). The CeN concentration was adjusted to 5 mmol/l and stored for later use. For experiments, the prediluted CeN-solution was added in different concentrations to the media in order to define a concentration suitable for the further experiments. For the further experiments, a concentration of 50 μmol/l was used.

2.5. Cell quantification assay

Cell quantification was performed with a 4′,6-diamidino-2-phenylindole (DAPI; Thermo Fisher Scientific, Dreieich, Germany) staining. After removal of the CCM, wells were washed once with Dulbecco's phosphate buffered Saline (DPBS, Thermo Fisher Scientific) before fixation with 100 μl 70 % ethanol (SERVA, Heidelberg, Germany) over 10 min. After removal of the ethanol, wells were dried for 30 min in a drying cabinet. Staining was performed for 5 min with 100 μl DAPI 1 μg/ml staining solution on a shaker at a low pace. After washing twice with 150 μl washing buffer, composing of aqua dest, 0.2 % Tween20 (Sigma-Aldrich), 500 mM NaCl, 20 mM Na-citrate (both Carl Roth, Karlsruhe, Germany), with pH adjusted to 5.0, the cell nucleus bound DAPI was eluted with 120 μl elution solution, composing of aqua dest, 20 mM Tris-HCL (Carl Roth), 2 % SDS (Thermo Fisher Scientific) with pH adjusted to 7.0, while shaking for 5 min. 100 μl per well was transferred to a white 96 well plate (Kisker Biotech, Steinfurt, Germany) and measured at 355/460 nm in a Wallac 1420 Victor 2 fluorescence reader (Perkin Elmer, Waltham, MA, USA).

2.6. Cell viability quantification assay

To quantify cell viability, a fluorescein diacetate (FDA) based assay was used [28]. After removal of CCM, cells were once washed with DBPS

before staining with 0.1 mg/ml FDA (Sigma Aldrich) in acetone (Carl Roth) diluted 1:50 in DPBS at 37°C for 5 min. After discarding the staining solution, cells were washed again before addition of 0.5 % Triton-X-100 (Sigma Aldrich) at 37°C for 5 min. Aliquots of the resulting lysates were transferred to a white 96 well plate and measured with a fluorescence microplate reader at 485/530 nm (ex/em).

2.7. Quantitative alkaline phosphatase (ALP) activity assay

The activity of ALP can be used as a marker for cellular differentiation towards osteoblasts [29]. ALP activity was quantified using the conversion of the ALP-substrate 4-methylumbelliferyl phosphate (4-MUP) in a fluorescence-based assay, following a previously published protocol [28]. Briefly described, the aliquots of the cell lysates also used for the FDA cell viability assay were incubated in a white 96 well microplate at 37°C for 15 min after adding 4-MUP substrate solution (composed of 100 μM 4-MUP (Life Technologies) in ALP assay buffer (75 mM TRIS pH 9.3, 1.5 mM $MgCl_2$ and 0.15 mM $ZnCl_2$, all Carl Roth)). A standard was provided using recombinant Shrimp ALP (Life Technologies). Measurements were performed on a fluorescence microplate reader with 485/535 nm (ex/em).

2.8. Quantitative and qualitative assessment of collagen formation

The amount of synthesized collagen within the primitive ECM was evaluated using Sirius Red staining, as it binds specifically to collagen [30–32], following a previously published protocol [7]. After removal of CCM, cells were washed with DBPS and fixated with ROTI Histofix and 4 % Formaldehyde (both Carl Roth) over 30 min at room temperature. After removing the fixate and thoroughly washing with aqua dest, cells were incubated 1 h while shaking with Sirius Red staining solution, composed of 1 mg/ml Sirius Red F3BA (Waldeck, Münster, Germany) in 1.3 % picric acid (Sigma Diagnostics, Livonia, MI, USA). After three washing steps with 0.01 M HCl (Carl Roth), pictures were taken with a Keyence BZ-X810 microscope (Keyence, Neu-Isenburg, Germany) at 10-fold magnification. The bound dye was then eluted with 0.1 M NaOH (Carl Roth) over 30 min at room temperature while shaking. Measurements of optical density were taken with a microplate reader (Autobio PHOmo, Zhengzhou, China) at 570 nm and referenced to a standard curve for quantification purposes.

2.9. Quantitative and qualitative assessment of calcium deposition

Calcification serves as a marker of ECM maturation. ECM calcification was assessed using an Alizarin Red S staining protocol, as it specifically binds to calcium deposits [33], following a previously described protocol [7]. Briefly described, after removal of CCM and washing the cells with aqua dest., cells were fixated with 70 % ethanol (SERVA) in aqua dest. at 6°C for 20 min. After removal of the fixate, cells were washed again once with aqua dest. before staining at room temperature for 10 min with Alizarin Red S staining solution, composed of 0.5 % Alizarin Red S (Waldeck) in aqua dest. After another washing step, pictures were taken with the Keyence BZ-X810 microscope at 10-fold magnification. The bound dye was then eluted with 10 % cetylpyridinumchloride 100 (Sigma Aldrich) solution containing 10 mM sodiumdihydrogenphosphate (AppliChem, Darmstadt, Germany). Measurements of optical density were taken with a microplate reader at 570 nm and quantified via normalization to a standard curve.

2.10. Analysis of lipid vacuole formation

After a washing step with 250 μl PBS cells were fixated in 200 μl 1 % ROTI Histofix (Carl Roth) over 30 min. After washing twice with aqua bidest, 200 μl Oil Red O Staining solution (3 mg/ml Oil Red O (Chroma-Gesellschaft, Münster, Germany) dissolved in 99 % Isopropanol) was added and incubated over 10 min at room temperature. After removal of the staining solution, wells were washed twice with 250 μl aqua bidest, once with 250 μl 70 % isopropanol and again with aqua bidest. Pictures were taken with the Keyence BZ-X810 microscope at 10-fold magnification. Aqua bidest was discarded and the staining solution eluted with 100 % isopropanol over 10 min while shaking. 100 μl Aliquots were transferred to a 96 well plate and measured in a Sunrise photometric reader (Tecan Austria, Grödig, Austria) at 490 nm, using 100 % isopropanol as blanks.

2.11. Gene expression analysis of adipogenesis, osteogenesis and ROS-related marker genes

The expression levels of genes encoding relevant markers for adipogenesis, osteogenesis and ROS-household were quantified via qPCR. Cell lysis was performed using PureLink RNA Mini Kit (Life Technologies). After isolating RNA from the cell lysates following the instructions from the manufacturer, 100 ng of RNA were reversely transcribed into cDNA with the High-Capacity RNA-to-cDNA-Kit (Life Technologies), following the manufacturer's protocol. Table 1 shows the primer pairs used for qPCR. Analyses were carried out in a LineGene 9600 Fluorescent Quantitative Detection System (Hangzhou BioER Technology, Hangzhou, China), using PowerUp SYBR Green Master Mix (Life Technologies). Gene expression levels were calculated using the ΔΔCt method under normalization to the endogenous reference gene tyrosine 3-monooxygenase/tryptophan 5-monooxygenase activation protein zeta (YWHAZ).

2.12. Intracellular ROS-detection with CellROX Green reagent

Intracellular ROS levels were detected using CellROX Green reagent. After removal of the medium, cells were incubated with 1 μl/ml CellROX Green Reagent (Life Technologies) in CCM over 1 h at standard cell culture conditions. After washing twice with PBS, cells were fixated with

Table 1
Primers used for qPCR and their associated biological function. Reference gene: tyrosine 3-monooxygenase/tryptophan 5-monooxygenase activation protein zeta (YWHAZ); marker for adipogenesis: lipoprotein lipase (LPL), fatty acid binding protein 4 (FABP4), peroxisome-proliferator-activated receptor gamma (PPARy); marker for osteogenesis: alkalic phosphatase (ALP), Collagen 1A1 (Col1A1), Osteocalcin (OCN), Osteoprotegerin (OPG); ROS-household-marker: Superoxiddismutase 2 (SOD2), Catalase (CAT), Glutathione Peroxidase 3 (GPX3), Forkhead-Box-O-1 transcription factor (FOXO1). AD: adipogenic differentiation, OD: osteogenic differentiation.

Gene	Forward (5' → 3')	Reverse (5' → 3')	Function
YWHAZ	TGC TTG CAT CCC ACA GAC TA	AGG CAG ACA ATG ACA GAC CA	Reference
LPL	CGC CGC CGA CCA AAG AAG A	AGG TAG CCA CGG ACT CTG C	AD
FABP4	TGG TTG ATT TTC CAT CCC AT	TAC TGG GCC AGG AAT TTG AC	AD
PPARy	TCC ATG CTG TTA TGG GTG AA	TCA AAG GAG TGG GAG TGG TC	AD
ALP	GCA CCT GCC TTA CTA ACT C	AGA CAC CCA TCC CAT CTC	OD
Col1A1	GTG GCC TGC CTG GTG AG	GCA CCA TCA TTT CCA CGA GC	OD
OCN	ACC GAG ACA CCA TGA GAG CC	GCT TGG ACA CAA AGG CTG CAC	OD
OPG	GGT CTC CTG CTA ACT CAG AAA GG	CAG CAA ACC TGA AGA ATG CCT CC	OD
SOD2	GGA GAT GTT ACA GCC CAG ATA GC	GCT TCC AGC AAC TCC CCT TT	ROS-scavenger
CAT	GTG CGG AGA TTC AAC ACT GCC A	CGG CAA TGT TCT CAC ACA GAC G	ROS-scavenger
GPX3	TAC GGA GCC CTC ACC ATT GAT G	CAG ACC GAA TGG TGC AAG CTC T	ROS-scavenger
FOXO1	CTT CAA GGA TAA GGG TGA CAG CAA C	TGG ATT GAG CAT CCA CCA AGA A	Sensor for oxidative stress

100 µl ROTI Histofix (Carl Roth) over 15 min at room temperature in darkness. Fixing solution was removed and after washing once with PBS, cells were incubated with 100 µl DAPI 1 µg/ml staining-solution over 5 min on a shaker. After washing once with washing solution (aqua dest, 500 mM NaCl, 20 mM Na-Citrate, 0.2 % Tween20, pH 5.0) and once with PBS afterwards, images were taken with the Keyence BZ-X810 microscope using green and blue channels at 10-fold magnification. An ImageJ macro was used to analyze the pictures with the operations Convert to 8 Bit, Invert, Set Threshold, Measure (% of total area). The threshold for DAPI pictures was set at 200, for CellROX Green pictures at 220 to filter background noise. When occurring, staining artifacts were manually unselected from the measured area using the rectangular image selection tool. DAPI nuclei-staining served as normalization to cell count, resulting CellROX Green/DAPI values describing the relative amount of intracellular ROS-positive area per cell. For comparison, a negative group with the potent anti-oxidant Ascorbic Acid (Sigma Aldrich) at 200 µl/ml in CCM and a positive group, treated with the pro-oxidant Tert-Butylhydroperoxide (Life Technologies) at 50 µl/ml in CCM were applied. Staining solution was added 1 h before adding CellROX Green reagent, as instructed by the manufacturer. For both settings, the AIM and the CCM setting, individual control groups were used in order to measure the wells on one and the same plate since the assay is very sensitive to light exposure making the comparison of different plate settings difficult.

2.13. Statistics

Statistical analysis was performed with IBM IPSS Statistics (Version 28, IBM, Armonk, NY, USA). Data values were compared by Kruskal-Wallis test, followed by Mann-Whitney *U* test. Statistical significance was determined for p-values < 0.05, and experiments were performed with $n = 6$ biological replicates, except for CellROX-Green Assay which was performed with $n = 4$ biological replicates. For each biological replicate in Alizarin Red S staining and Sirius Red staining, two technical replicates were measured and the average value per biological replicate used for statistical analysis. Graphs were designed in Microsoft Excel and show mean values with standard deviations.

3. Results

3.1. Definition of a CeN concentration for the experiments

The addition of CeN increased cell proliferation on D7 and D14 significantly in the higher concentrations (Fig. 1a) compared to the groups with CCM and those that were cultivated in presence of less than 50 µmol/l CeN. On D7, viability was significantly increased in presence of CeN in higher concentrations, while on D14 the average concentrations led to a decrease in viability (Fig. 1b). Based on these findings, a CeN concentration of 50 µmol/l was selected for the further experiments.

3.2. CeN enhances ECM formation, maturation and osteogenic differentiation

Compared to the CCM-group, CeN significantly increased collagen deposition on D14 and D21 (Fig. 2a, c) and ECM calcification on D14 compared to the CCM group (Fig. 2b, d). Also, the presence of CeN sinificantly increased ALP activity on both D7 and D14 (Fig. 2e).

The expression levels of the genes encoding for OCN (Fig. 3a) and OPG (Fig. 3b) were significantly upregulated in the CeN group on D14, OCN also already on D7. ALP gene expression was significantly down-regulated on D14 (Fig. 3c), while Col1A1 was significantly down-regulated on both days (Fig. 3d).

3.3. CeN suppresses adipogenic differentiation and adipogenesis

The presence of CeN reduced lipid production significantly on D7 in comparison to the AIM group – CeN even suppressed the lipid vaculoe

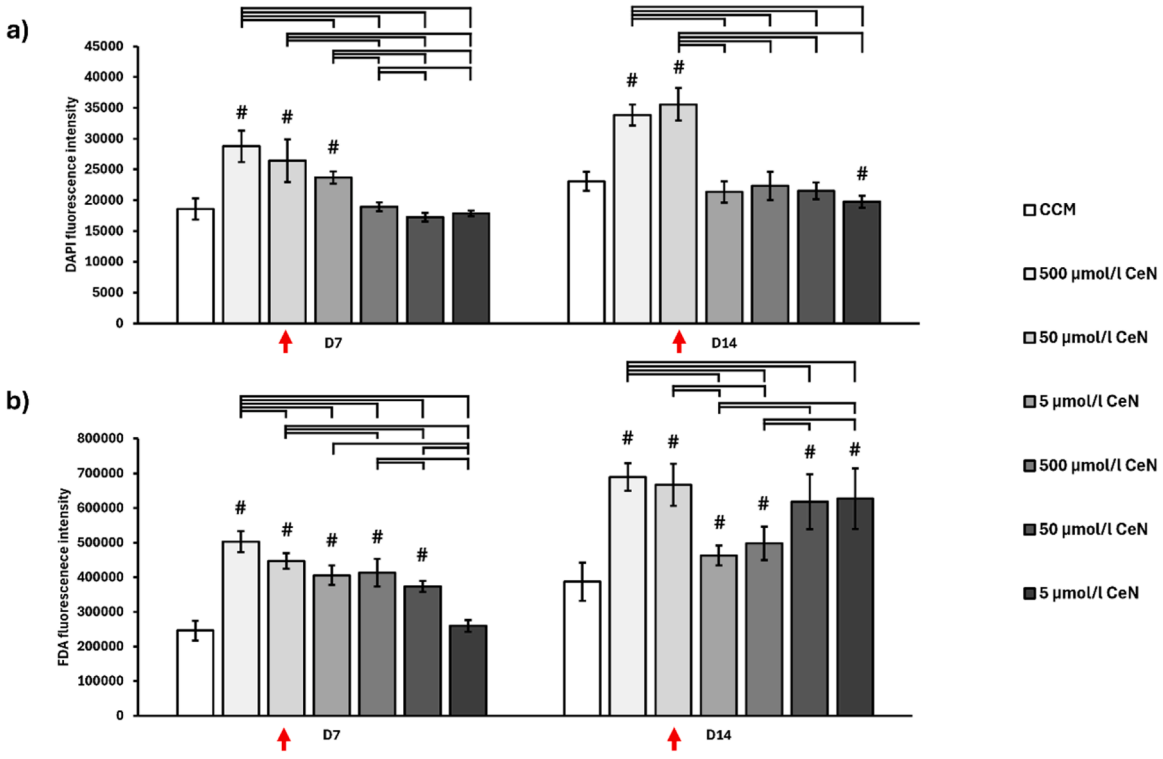

Fig. 1. Quantification of cell proliferation (a) and cell viability (b) on D7 and D14 in a concentration dependant manner. (#) marks significant differences to the CCM-group, significant differences between two groups are marked with brackets encompassing the respective groups. The concentration of 50 µmol/l is used for the further experiments and therefore highlighted by a red arrow.

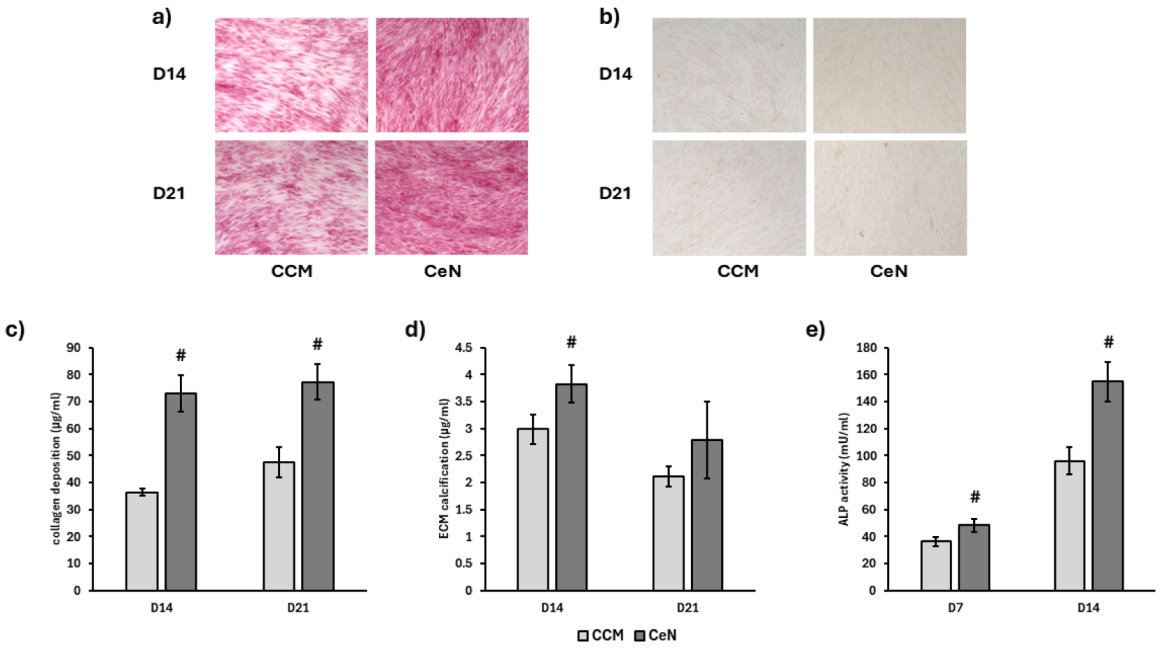

Fig. 2. Representative microscopy pictures of stainings detecting collagen formation (a; red = collagen deposits) and calcium deposition (b; red = calcium deposits), magnification 10-fold. Quantification of collagen formation (c), calcium deposits (d) and ALP activity (e). Assays shown on D7 and D14. (#) marks significant differences to the CCM-group.

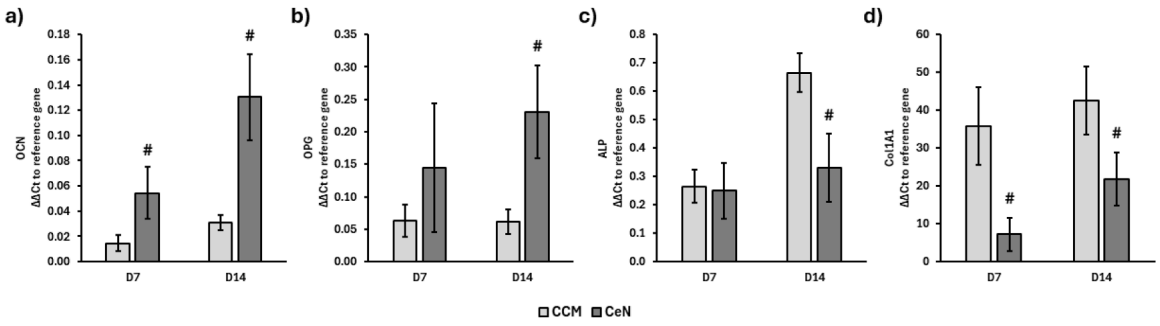

Fig. 3. Expression levels of the osteogenic marker genes OCN (a), OPG (b), ALP (c) and Col1A1 (d) on D7 and D14. (#) marks significant differences from the CCM-group.

formation to a non-significant difference compared to the ("non-adipogenic") CCM control group (Fig. 4a, b). No significant differences were detected on D14 between the CeN and the AIM groups. On a gene expression level, the adipogenesis marker genes were downregulated on D14 in comparison to the AIM group, while LPL expression was also significantly reduced on D7 (Fig. 4c-e). As expected, the presence of AIM led to a significant upregulation of the adipogeic marker genes compared to the CCM group on D7 and D14.

3.4. CeN reduces physical presence of ROS and modulates ROS-associated gene expression

The presence of CeN significantly reduced the physical presence of ROS compared to the CCM group on D7 and D14 (Fig. 5a, b). In AIM, the presence of CeN numerically reduced ROS on D7 and D14 (Fig. 5c, d).

On a genetic level, in the conventional CCM-based setting, CeN significantly upregulated SOD2 on both days and GPX3 on D14, while it had no significant or numerical impact on CAT or FOXO1 (Fig. 6a-d). In the presence of AIM (Fig. 6e-h), CeN significantly increased SOD2 expression compared to the AIM group on D7 which was significantly downregulated compared to the CCM group. On D14, SOD2 was significantly upregulated in both AIM-groups compared to the CCM group – no suppressing effects of CeN in the AIM setting could be observed. GPX3-expression was significantly increased in the CeN-group compared to CCM on D14. FOXO and CAT were downregulated in the presence of CeN when compared to the AIM group on D7 and D14.

4. Discussion

IM-approaches have recently gained increasing attention in BTE-associated research, especially associated with biomaterials [1,4,34]. Biomaterials can serve as a local delivery vehicle to provide the biologically active ions to their intended site of action [35,36]. Several metallic ions have been investigated for their suitability to improve the biological functions of biomaterials for BTE-applications – one promising ion is cerium that has not only been shown to enhance osteogenic differentiation of bone precursor cells in various settings [7,8,10,15,16] but also serves as a self-regenerating ROS-scavenger [37]. The latter property is particularly interesting since BMSCs, that constitute the cell pool for osteoblast development, are not only able to differentiate into osteoblasts but can also differentiate into an undesired adipogenic pathway, eventually resulting in adipocytes that are not useful for bone regeneration [38]. The presence of ROS favors adipogenic over osteogenic differentiation in BMSCs [14,39,40]. Therefore, the local presence

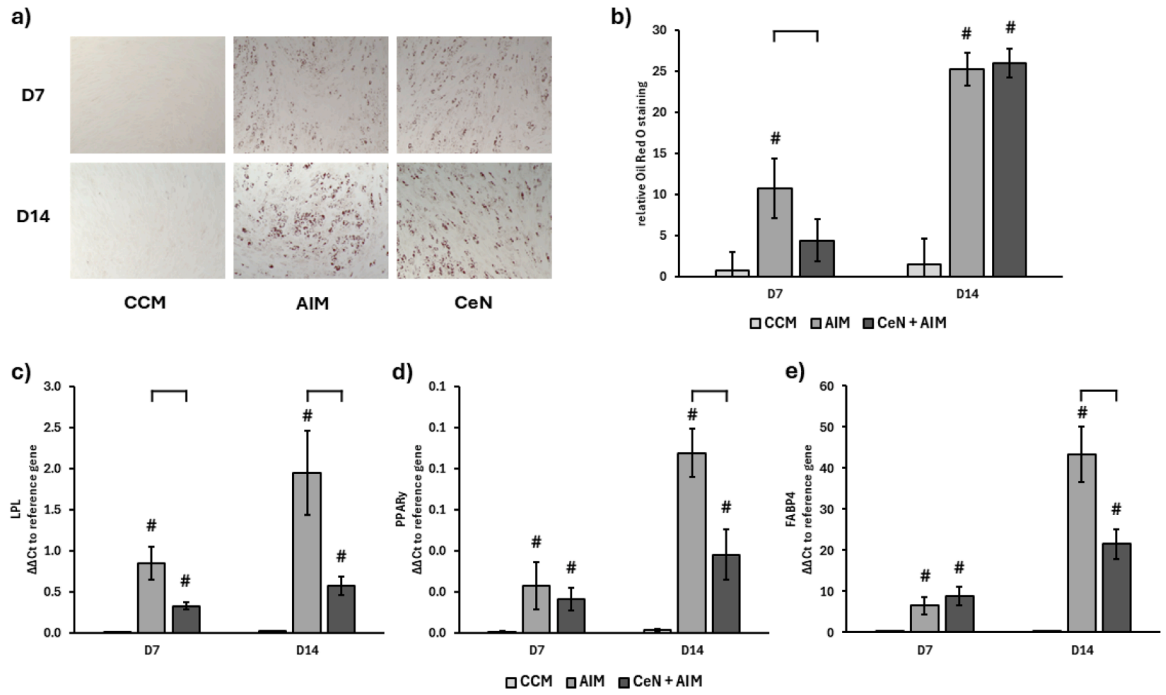

Fig. 4. Representative microscopy pictures of red-stained lipid vacuoles (a), magnification 10-fold. Quantification of lipid content (b), gene expression of PPARγ (c), FABP4 (d) and LPL (e) on D7 and D14. (#) marks significant differences to the CCM-group, significant differences between two groups are marked with brackets encompassing the respective groups.

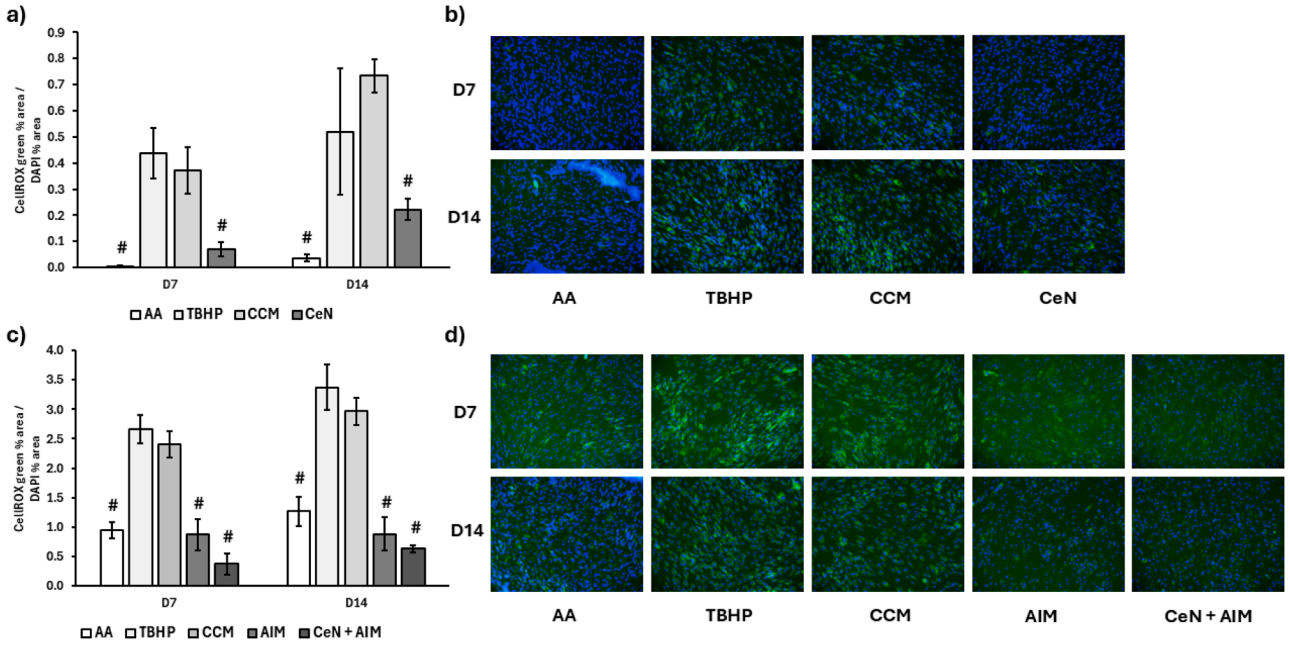

Fig. 5. Quantification of relative area with positive ROS-signal, normalized on cell count in the conventional (a) and adipogenic (c) setting on D7 and D14. Corresponding fluorescence microscopy pictures of ROS-detection and cell nuclei staining the conventional (a) and adipogenic (c) setting on D7 and D14; ROS-signal in green, cell nuclei in blue, magnification 10-fold. (#) marks significant differences to the CCM-group.

of a ROS-suppressing ion like cerium might help to favor osteogenic over adipogenic differentiation in BMSCs via a reduction of ROS – this hypothesis was investigated within the present study.

In this study, CeN ($Ce(NO_3)_3$) was used as Ce-source since it is commonly used for the synthesis of Ce-doped biomaterials [7,9,21]. In order to assess the cytocompatibility of CeN, its effects on the viability and proliferation of BMSCs were assessed at different concentrations. The higher concentrations not only proved to be non-toxic but improved viability and proliferation significantly. While the step from 5 μM to 50 μM showed an increase in both viability and proliferation, a further 10-fold increase to 500 μM showed less of a significant impact, hence the concentration used for all tests was chosen at 50 μM. While Hu and co-workers reported that $CeCl_2$ increased the viability of mouse BMSCs at lower concentrations, they described a decreasing effect on cell viability at higher concentrations of 10 μM – which is, compared to this study, a rather low concentration [15]. Even the presence of CeN at

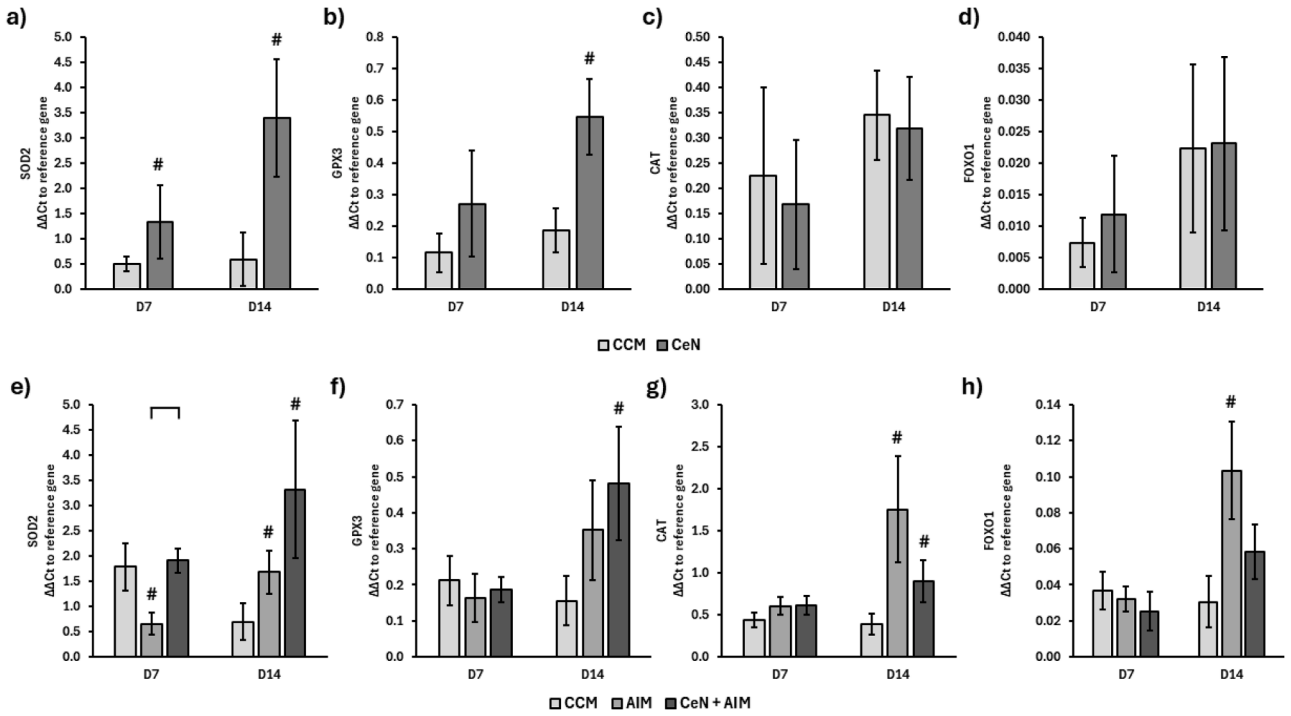

Fig. 6. ROS-associated gene expression in the conventional (CCM; a-d) and AIM (e-h) setting. Expression of SOD2 (a, e), GPX3 (b, f), CAT (c, g) and FOXO1 (d, h) are shown on D7 and D14. (#) marks significant differences to the CCM-group, significant differences between two groups are marked with brackets encompassing the respective groups.

50 μM in this study was not only cytocompatible but even enhanced the viability and proliferation of BMSCs. The differences in the study of Hu et al. might be explained by the different cells used (human vs. mouse) and the different molecules ($Ce(NO_3)_3$ vs. $CeCl_2$). Similar positive effects on cell viability and proliferation for Ce-doped biomaterials have been described before [7,17,21].

Within this study's experimental setting only one cell type, namely BMSCs, was used. The osteogenic differentiation of BMSCs can be assessed on different levels, that are (i) the cellular level by analyzing the actual cellular differentiation from BMSCs along the osteogenic lineage finally resulting in mature osteoblasts, (ii) the cellular genetic level by analyzing the expression patterns of genes involved in the development from BMSCs to osteoblasts and (iii) the matrix level, focusing on analyzing the formation and maturation of the primitive osseous ECM that is created during maturation of the cell layers [29]. Osteoblasts produce ALP in order to provide inorganic phosphate that is used to enhance ECM mineralization [41]. The ALP activity can therefore be assessed as a direct correlate of the differentiation status of the BMSCs towards osteoblasts: the presence of CeN significantly increased ALP activity on D14 compared to the CeN-free CCM control group. The ALP activity levels are expected to peak after 10–14 days after the start of the cultivation period within the used setting [29], going well in line with the observed development of ALP activity. Our group previously reported on similar observations regarding the influence of Ce-doped mesoporous bioactive glass nanoparticles (MBGNs) on BMSCs [7]. Similar ALP activity patterns in a setting using $CeCl_2$ and murine BMSCs were also described by Hu et al. [15]. On a genetic level, the presence of CeN led to a decrease in the expression of the gene encoding for ALP on D14 – even though, the enzyme was more active in the CeN-group. Possible explanations for these observations might be post-translational modifications that lead to a significant difference between mRNA expression and resulting concentration of the encoded proteins [42]. Also, the patterns of gene expression levels can change quickly, depending on cell metabolism, cell growth, differentiation and many further factors [43]. The ECM formation and maturation (i.e. calcification) was improved in the presence of CeN. Luo and co-workers reported on very similar findings when analyzing the effects of Ce-oxide nanoparticles on mouse bone precursor cells [20]: the positive effects on the ECM are mediated by an activation of the Wnt pathway. Comparable to the observed differences between ALP activity and gene expression patterns, also the Col1A1 gene expression was downregulated in the presence of CeN while the collagen content was increased. Possible explanations are already given above. However, the expression patterns of the two other genes that are upregulated during osteogenic differentiation, namely OCN and OPG were stimulated by CeN. Similar observations for OCN gene expression were reported by Liu et al. and attributed to the involvement of the TGF-β/BMP signaling pathway [16]. Hu reported on an upregulation of OCN gene expression via Smad-pathways [15]. This shows that Ce is involved in different pathways that result in increased osteogenic differentiation processes within BMSCs. These pathways, that are regulated by Ce during osteogenic differentiation, should be assessed further in order to understand the mechanisms leading to molecular effects of Ce on BMSCs in greater detail.

BMSCs are able to differentiate into adipogenic lineage [38]. This way of differentiation is undesired in BTE settings. In this study, not only the presence of lipid vacuoles in an adipogenic differentiation enhancing setting but also the level of adipogenic gene expression were downregulated in presence of CeN. Similar findings have been reported before. For example, Zhang and co-workers described suppressing effects of cerium-containing nanoparticles (nanoceria) on the adipogenic differentiation of mouse BMSCs [8]. Rocca and co-workers also reported similar effects of nanoceria on rat-dervied BMSCs [17]. Very similar anti-adipogenic effects were recently described in a study conducted by our group using Ce-doped MBGNs in a setting including BMSCs – however, the effects on osteogenic differentiation have not been investigated within the same experimental setting [11]. Notably, the anti-adipogenic effects shown in the present study on lipid vacuole formation were limited to D7 while the presence of CeN did not yield a sustained suppression of lipid vacuole formation on D14. This shows that the early differentiation of BMSCs might be influenced positively, i.e. not into

adipoigenic direction. Also, the effects of CeN on a genetic level persist until D14. Independently from these effects in simple cell culture settings only involving one cell type, there are even reports available of a systemic effect of nanoceria on obesity: nanoceria that has been injected intraperitoneally in rats reduced their weight gain in comparison to the untreated control group [44]. There is strong evidence that Ce interacts with the earliest mechanisms of adipogenic differentiation: PPARγ, a key player of adipogenic differentiation, that acts by mediating cellular differentiation into adipocytes by different downstream effectors like FABP4 or LPL [45,46] has been downregulated in presence of Ce in this study and in other studies before [17,44]. The underlying molecular mechanisms have not yet been clarified. In order to gain a better understanding of these processes, future studies should look deeper into these processes. It should be also elucidated possible different effects of ceria nanoparticles as opposed to Ce ions being released from a carrier and acting as dissolution products in cell culture medium.

One possible factor that leads to enhancement and stimulation of adipogenic differentiation is the presence of ROS [13,14,39,40]. The enhancing effects of Ce on osteogenic differentiation and the suppressing effects on adipogenic differentiation as shown in this study and other studies [7, 8, 10, 15–18, 20] might therefore be explained by the influence of Ce on ROS presence. However, so far, there is only indirect evidence available about the antioxidant effects of Ce. For example, Zheng and co-workers described an upregulation of anti-oxidant gene expression when the macrophage cell line J774a.1 was exposed to Ce-doped MBGNs [9]. In the present study, not only the effects of CeN on the activity of genes encoding for ROS-scavenging enzymes like SOD2, CAT and GPX3 were assessed, but also the impact of CeN on the actual physical presence and activity of ROS. While the impact of CeN on the expression patterns of genes that are involved in ROS metabolism was comparable to those described before [47], the presence of CeN reduced ROS activity in the CCM-group significantly and in the AIM setting numerically. This data shows that CeN has a major impact on the presence of ROS and their impact on the ROS-affiliated gene expression profiles. For the first time, this study analyzed the actual impact of Ce ions on the physical presence of ROS. Since the presence of ROS is linked to the differentiation fate of BMSCs, the modulation of ROS presence and activity might (in parts) explain the pro-osteogenic and anti-adipogenic effects of Ce. However, a more detailed understanding of the molecular actions of Ce in the differentiation process of BMSCs is needed to elcuidate the extent to which the antioxidant properties play a role in regulating the differentiation pathways. In addition, possible “nano” effects induced by nanoceria must be considered, to differentiate such effects from ionic influence provided by Ce ions, as investigated in this work.

5. Conclusions

The presence of CeN improved viability, enhanced proliferation, and reduced ROS-levels in BMSCs. Furthermore, CeN was able to affect the differentiation patterns of BMSCs: when CeN was added to the cell culture, especially the early stages of adipogenic differentiation were suppressed while osteogenic differentiation was enhanced. Also, the formation and maturation of a primitive ECM were enhanced in the CeN-containing settings. The presence of CeN reduced the physical presence of ROS – the gene expression profiles of the BMSCs shifted towards an anti-oxidant profile. Although, to the best knowledge of the authors, there is no Ce-containing material approved for clinical use available on the market so far, Ce ions are promising for application in IM-guided BTE, especially as a part of the chemical composition of biomaterials (e.g. BGs) that serve as vectors to provide Ce locally at the anticipated site of action. Further research is necessary including in-vivo experiments to clarify the biological mechanisms and pathways that are involved in the Ce-mediated modulation of BMSC differentiation, also to categorize the role its ROS-suppressing, antioxidant effects on the fate and direction of cellular differentiation.

Disclosure

This study was funded by the research grant of the Heidelberg Orthopedic University Hospital and by a grant of the Körperschaftsvermögen der Universität Heidelberg from Dres. Majic/Majic-Schlez-Foundation (grant number: 3541.29). The authors declare that there are no conflicts of interest in regard to this study. This study contains parts of Valentin Jacobsen’s doctoral thesis.

Ethics statement

This protocol of the study strictly followed the contents of the declaration of Helsinki in its present form. Patients were informed prior to material collection and gave written consent for the collection. The responsible ethics committee of the Medical Faculty of Heidelberg University approved the harvesting of patient tissue samples, isolation and cultivation of cells used for this study (S-340/2018).

Declaration of Competing Interest

The authors hereby declare that they do not have relevant Conflicts of Interest in relation to the submitted work entitled “Insights into ionic medicine: Cerium reduces the presence of reactive oxygen species and favors osteogenic over adipogenic differentiation in human mesenchymal stromal cells” that is submitted for consideration in *Journal of Trace Elements in Medicine and Biology*.

References

[1] H.-H. Lu, D. Ege, S. Salehi, A.R. Boccaccini, Ionic medicine: Exploiting metallic ions to stimulate skeletal muscle tissue regeneration, Acta Biomater. 190 (2024) 1–23.
[2] A.R. Amini, C.T. Laurencin, S.P. Nukavarapu, Bone tissue engineering: recent advances and challenges, Crit. Rev. Biomed. Eng. 40 (5) (2012) 363–408.
[3] S. Li, Y. Cui, H. Liu, Y. Tian, G. Wang, Y. Fan, et al., Application of bioactive metal ions in the treatment of bone defects, J. Mater. Chem. B 10 (45) (2022) 9369–9388.
[4] U. Pantulap, M. Arango-Ospina, A.R. Boccaccini, Bioactive glasses incorporating less-common ions to improve biological and physical properties, J. Mater. Sci. Mater. Med 33 (1) (2021) 3.
[5] S. Wilkesmann, F. Westhauser, Tailoring the Osteogenic Properties of Bioactive Glasses by Incorporation of Therapeutic Ions for Orthopedic Applications, Bioact. Glass Glass-Ceram. (2022) 203–226.
[6] F. Westhauser, B. Widholz, Q. Nawaz, S. Tsitlakidis, S. Hagmann, A. Moghaddam, et al., Favorable angiogenic properties of the borosilicate bioactive glass 0106-B1 result in enhanced in vivo osteoid formation compared to 45S5 Bioglass, Biomater. Sci. 7 (12) (2019) 5161–5176.
[7] F. Westhauser, F. Rehder, S. Decker, E. Kunisch, A. Moghaddam, K. Zheng, et al., Ionic dissolution products of Cerium-doped bioactive glass nanoparticles promote cellular osteogenic differentiation and extracellular matrix formation of human bone marrow derived mesenchymal stromal cells, Biomed. Mater. 16 (3) (2021).
[8] Q. Zhang, K. Ge, H. Ren, C. Zhang, J. Zhang, Effects of Cerium Oxide Nanoparticles on the Proliferation, Osteogenic Differentiation and Adipogenic Differentiation of Primary Mouse Bone Marrow Stromal Cells In Vitro, J. Nanosci. Nanotechnol. 15 (9) (2015) 6444–6451.
[9] K. Zheng, E. Torre, A. Bari, N. Taccardi, C. Cassinelli, M. Morra, et al., Antioxidant mesoporous Ce-doped bioactive glass nanoparticles with anti-inflammatory and pro-osteogenic activities, Mater. Today Bio 5 (2020) 100041.
[10] G. Zhou, G. Gu, Y. Li, Q. Zhang, W. Wang, S. Wang, et al., Effects of cerium oxide nanoparticles on the proliferation, differentiation, and mineralization function of primary osteoblasts in vitro, Biol. Trace Elem. Res 153 (1-3) (2013) 411–418.
[11] V. Jacobsen, E. Kunisch, C. Merle, B. Xue, K. Zheng, T. Renkawitz, et al., Cerium-doped mesoporous bioactive glass nanoparticles reduce oxidative stress and adipogenic differentiation in human bone marrow-derived mesenchymal stromal cells, J. Trace Elem. Med Biol. 88 (2025) 127617.
[12] B.C. Nelson, M.E. Johnson, M.L. Walker, K.R. Riley, C.M. Sims, Antioxidant Cerium Oxide Nanoparticles in Biology and Medicine, Antioxid. (Basel) 5 (2) (2016).
[13] F. Atashi, A. Modarressi, M.S. Pepper, The role of reactive oxygen species in mesenchymal stem cell adipogenic and osteogenic differentiation: a review, Stem Cells Dev. 24 (10) (2015) 1150–1163.
[14] D. de Villiers, M. Potgieter, M.A. Ambele, L. Adam, C. Durandt, M.S. Pepper, The Role of Reactive Oxygen Species in Adipogenic Differentiation, Adv. Exp. Med Biol. 1083 (2018) 125–144.
[15] Y. Hu, Y. Du, H. Jiang, G.-S. Jiang, Cerium promotes bone marrow stromal cells migration and osteogenic differentiation via Smad1/5/8 signaling pathway, Int J. Clin. Exp. Pathol. 7 (8) (2014) 5369–5378.
[16] D.D. Liu, J.C. Zhang, Q. Zhang, S.X. Wang, M.S. Yang, TGF-beta/BMP signaling pathway is involved in cerium-promoted osteogenic differentiation of mesenchymal stem cells, J. Cell Biochem 114 (5) (2013) 1105–1114.

[17] A. Rocca, V. Mattoli, B. Mazzolai, G. Ciofani, Cerium oxide nanoparticles inhibit adipogenesis in rat mesenchymal stem cells: potential therapeutic implications, Pharm. Res 31 (11) (2014) 2952–2962.
[18] J. Zhang, C. Liu, Y. Li, J. Sun, P. Wang, K. Di, et al., Effect of cerium ion on the proliferation, differentiation and mineralization function of primary mouse osteoblasts in vitro, J. Rare Earths 28 (1) (2010) 138–142.
[19] K. Li, Q. Shen, Y. Xie, M. You, L. Huang, X. Zheng, Incorporation of cerium oxide into hydroxyapatite coating regulates osteogenic activity of mesenchymal stem cell and macrophage polarization, J. Biomater. Appl. 31 (7) (2017) 1062–1076.
[20] J. Luo, S. Zhu, Y. Tong, Y. Zhang, Y. Li, L. Cao, et al., Cerium Oxide Nanoparticles Promote Osteoplastic Precursor Differentiation by Activating the Wnt Pathway, Biol. Trace Elem. Res 201 (2) (2023) 865–873.
[21] I. Atkinson, E.M. Anghel, S. Petrescu, A.M. Seciu, L.M. Stefan, O.C. Mocioiu, et al., Cerium-containing mesoporous bioactive glasses: Material characterization, in vitro bioactivity, biocompatibility and cytotoxicity evaluation, Microporous Mesoporous Mater. 276 (2019) 76–88.
[22] B. Widholz, S. Tsitlakidis, B. Reible, A. Moghaddam, F. Westhauser, Pooling of Patient-Derived Mesenchymal Stromal Cells Reduces Inter-Individual Confounder-Associated Variation without Negative Impact on Cell Viability, Proliferation and Osteogenic Differentiation, Cells 8 (6) (2019).
[23] B. Reible, G. Schmidmaier, A. Moghaddam, F. Westhauser, Insulin-Like Growth Factor-1 as a Possible Alternative to Bone Morphogenetic Protein-7 to Induce Osteogenic Differentiation of Human Mesenchymal Stem Cells in Vitro, Int J. Mol. Sci. 19 (6) (2018).
[24] B. Reible, G. Schmidmaier, M. Prokscha, A. Moghaddam, F. Westhauser, Continuous stimulation with differentiation factors is necessary to enhance osteogenic differentiation of human mesenchymal stem cells in-vitro, Growth Factors 35 (4-5) (2017) 179–188.
[25] Y.K. Yang, C.R. Ogando, C. Wang See, T.Y. Chang, G.A. Barabino, Changes in phenotype and differentiation potential of human mesenchymal stem cells aging in vitro, Stem Cell Res Ther. 9 (1) (2018) 131.
[26] M. Moll, A. Scheurle, Q. Nawaz, T. Walker, E. Kunisch, T. Renkawitz, et al., Osteogenic and angiogenic potential of molybdenum-containing mesoporous bioactive glass nanoparticles: An ionic approach to bone tissue engineering, J. Trace Elem. Med. Biol. 86 (2024) 127518.
[27] J.D. Kretlow, Y.-Q. Jin, W. Liu, W.J. Zhang, T.-H. Hong, G. Zhou, et al., Donor age and cell passage affects differentiation potential of murine bone marrow-derived stem cells, BMC Cell Biol. 9 (1) (2008) 60.
[28] S. Wilkesmann, F. Westhauser, J. Fellenberg, Combined Fluorescence-Based in Vitro Assay for the Simultaneous Detection of Cell Viability and Alkaline Phosphatase Activity during Osteogenic Differentiation of Osteoblast Precursor Cells, Methods Protoc. 3 (2) (2020).
[29] E. Birmingham, G.L. Niebur, P.E. McHugh, G. Shaw, F.P. Barry, L.M. McNamara, Osteogenic differentiation of mesenchymal stem cells is regulated by osteocyte and osteoblast cells in a simplified bone niche, Eur. Cell Mater. 23 (2012) 13–27.
[30] Sweat F, Puchtler H, Rosenthal SI. Sirius Red F3ba as a Stain for Connective Tissue, Arch. Pathol. 78 (1964) 69–72.
[31] B.J. Walsh, S.C. Thornton, R. Penny, S.N. Breit, Microplate reader-based quantitation of collagens, Anal. Biochem 203 (2) (1992) 187–190.
[32] L.C. Junquiera, L.C. Junqueira, R.R. Brentani, A simple and sensitive method for the quantitative estimation of collagen, Anal. Biochem 94 (1) (1979) 96–99.
[33] H. Puchtler, S.N. Meloan, M.S. Terry, On the history and mechanism of alizarin and alizarin red S stains for calcium, J. Histochem Cytochem 17 (2) (1969) 110–124.
[34] A. Hoppe, N.S. Guldal, A.R. Boccaccini, A review of the biological response to ionic dissolution products from bioactive glasses and glass-ceramics, Biomaterials 32 (11) (2011) 2757–2774.
[35] A. Shearer, M. Montazerian, J.C. Mauro, Modern definition of bioactive glasses and glass-ceramics, J. Non-Cryst. Solids 608 (2023) 122228.
[36] M.B. Taye, Biomedical applications of ion-doped bioactive glass: a review, Appl. Nanosci. 12 (12) (2022) 3797–3812.
[37] J.T. Dahle, Y. Arai, Environmental geochemistry of cerium: applications and toxicology of cerium oxide nanoparticles, Int J. Environ. Res Public Health 12 (2) (2015) 1253–1278.
[38] S.S. Liu, X. Fang, X. Wen, J.S. Liu, M. Alip, T. Sun, et al., How mesenchymal stem cells transform into adipocytes: Overview of the current understanding of adipogenic differentiation, World J. Stem Cells 16 (3) (2024) 245–256.
[39] N. Puri, K. Sodhi, M. Haarstad, D.H. Kim, S. Bohinc, E. Foglio, et al., Heme induced oxidative stress attenuates sirtuin1 and enhances adipogenesis in mesenchymal stem cells and mouse pre-adipocytes, J. Cell Biochem 113 (6) (2012) 1926–1935.
[40] M. Higuchi, G.J. Dusting, H. Peshavariya, F. Jiang, S.T. Hsiao, E.C. Chan, et al., Differentiation of human adipose-derived stem cells into fat involves reactive oxygen species and Forkhead box O1 mediated upregulation of antioxidant enzymes, Stem Cells Dev. 22 (6) (2013) 878–888.
[41] S. Vimalraj, Alkaline phosphatase: Structure, expression and its function in bone mineralization, Gene 754 (2020) 144855.
[42] C. Vogel, E.M. Marcotte, Insights into the regulation of protein abundance from proteomic and transcriptomic analyses, Nat. Rev. Genet 13 (4) (2012) 227–232.
[43] T. Maier, M. Güell, L. Serrano, Correlation of mRNA and protein in complex biological samples, FEBS Lett. 583 (24) (2009) 3966–3973.
[44] A. Rocca, S. Moscato, F. Ronca, S. Nitti, V. Mattoli, M. Giorgi, et al., Pilot in vivo investigation of cerium oxide nanoparticles as a novel anti-obesity pharmaceutical formulation, Nanomedicine 11 (7) (2015) 1725–1734.
[45] K. Schoonjans, J. Peinado-Onsurbe, A.M. Lefebvre, R.A. Heyman, M. Briggs, S. Deeb, et al., PPARalpha and PPARgamma activators direct a distinct tissue-specific transcriptional response via a PPRE in the lipoprotein lipase gene, EMBO J. 15 (19) (1996) 5336–5348.
[46] E.D. Rosen, O.A. MacDougald, Adipocyte differentiation from the inside out, Nat. Rev. Mol. Cell Biol. 7 (12) (2006) 885–896.
[47] J. Colon, N. Hsieh, A. Ferguson, P. Kupelian, S. Seal, D.W. Jenkins, et al., Cerium oxide nanoparticles protect gastrointestinal epithelium from radiation-induced damage by reduction of reactive oxygen species and upregulation of superoxide dismutase 2, Nanomedicine 6 (5) (2010) 698–705.